

CATALOGUE OF LUNAR THERMAL ANOMALIES. Y.C. ZHENG^{1,2,3}, K.L. CHAN², K.T. TSANG², Y.C. ZHU¹, G.P. HU³, Y.L. ZOU¹, Z.Y. OUYANG¹, ¹National Astronomical Observatories, Chinese Academy of Sciences (A20 Datun Rd., Chaoyang, Beijing 100012, China. zyc@nao.cas.cn and maklchan@ust.hk); ²Centre for Space Science Research and Department of Mathematics, The Hong Kong University of Science and Technology; ³Space Science Institute, Macau University of Science and Technology.

Introduction: The scene on the night-time lunar surface is still poorly understood until today, making it an curious and attractive topic for the astronomers and the general public. Without heat preservation by atmosphere like as on the Earth, the lunar surface cools rapidly during lunar night or lunar eclipse¹. However, the heating and cooling rate of the lunar surface is not uniform. Many ground-based observations in microwave (MW) and infrared (IR) band have revealed that some areas on the Moon cool much slowly or rapidly than the surroundings, which resulted as hot spots or cold spots on the Moon. In infrared observation from the Earth, the entire disk during lunar total eclipse dotted by hundreds of "hot spots"².

Data and Method: The new observation data sets of the Moon give us a chance to renew our understandings of the lunar thermal anomalies. The MW and IR observation data sets are much benefit to this research. The MW observations were carried by China's Chang'E-1 (CE-1) and Chang'E-2 (CE-2) in 2007 and 2010, respectively. The infrared observation was carried by LRO Diviner radiometer³. We have discovered many cold spots on the nighttime lunar surface in CE-1's observation⁴. In this paper, we will present the complete catalogue of lunar thermal anomalies discovered from the recent CE-2 observation. The thermal anomalies have been corroborate verified between CE-1's and CE-2's MW data. Diviner's nighttime surface temperature and the image data are integrated by GIS software. We hope to classify the different thermal anomalies, to understand their correlation with surface temperature and geologic features.

Results and Discussion: Generally, thermal anomalies is described as those regions where is colder or warmer than the surroundings. If the center TB (TB_{cent}) is higher than the surrounding TB (TB_{surr}), these regions should be identified as hot spots. Otherwise, the regions with lower center TB should be identified as cold spots. It is necessary to give a subjective threshold value to define the cold spots or hot spots. In this paper, we define 3 K as a rational threshold value.

The 37 GHz nighttime image is used to construct the catalogue of thermal anomalies. We use the microwave image to produce a contour map (Fig. 1). On the interval of 0.5K contour map, the thermal anomalies were shown as multi-ring patches or spots. The TB value of the outermost ring was treated and extracted as

TB_{surr} , the TB within the centre ring was treated and extracted as TB_{cent} . $\Delta TB = TB_{surr} - TB_{cent}$, stands for the abnormal degree of the thermal anomalies. We identified 266 thermal anomalies. Among them, 244 are cold spots, 22 are hot spots in the nighttime microwave map.

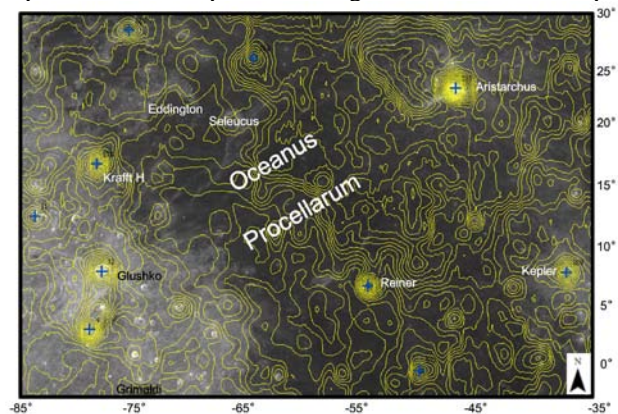


Fig. 1. Identification of microwave thermal anomalies on the Moon. Total 266 thermal anomalies are identified from the contour Map of TB.

TB_{surr} , TB_{cent} , ΔTB in four frequency channels at lunar noon and midnight were loaded into the catalogue. Then the auxiliary information, i.e. the latitude and longitude in the center, the size and area, the standard deviation of TB data in the anomalies, were also loaded. The full catalogue with detail information will be published as soon.

All lunar thermal anomalies in the range of N60° to S60° are shown on the visible image (Fig. 2). The distribution density of anomalies in the highland are higher than those in the maria. The maria are covered by the homogeneous basaltic material with similar thermal properties. In addition, the maria are characterized by their smooth topography and low density of craters which lead to relative uniform thermal performance in the maria.

In order to understand the factors to cause thermal anomalies on the Moon, we combined the different data sets to study the correlation between their visible image, microwave TB map and infrared observation. The data sets include the CE-2's and LRO WAC's visible image, 37GHz daytime and nighttime TB data, and the Diviner infrared data which is corresponding the surface temperature well. According to the correspond-

ing topographic features, the 266 thermal anomalies in our catalogue, including cold spots and hot spots, could

be classified as five types (Table 1).

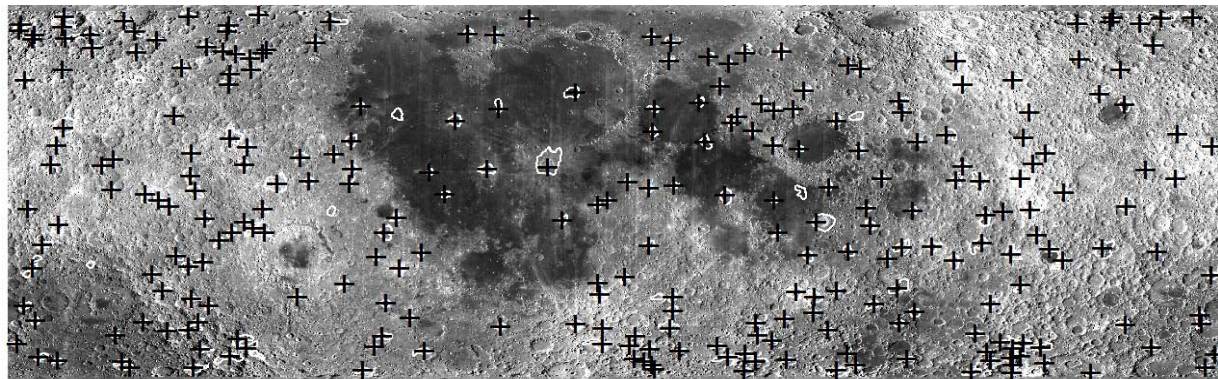


Fig. 2 The distribution of lunar thermal anomalies in the range of N60° to S60°

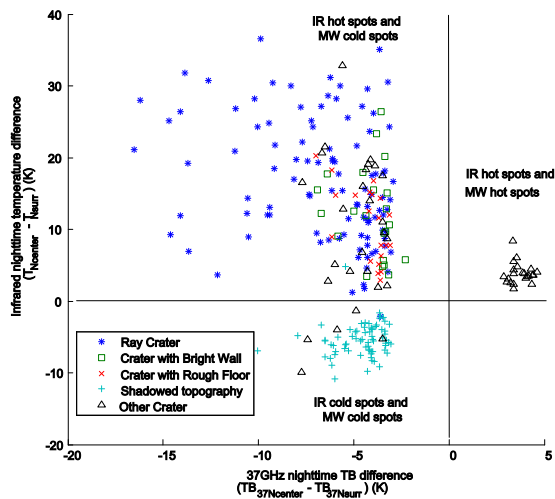


Fig. 3. The performance of thermal anomalies in nighttime microwave map and infrared maps. X axis: the 37GHz ΔTB . Y axis: the infrared temperature difference between the center and surrounding. The negative values means cold spots. The positive value means hot spots.

The characteristics of thermal anomalies in the MW and IR observations, and their corresponding topographic features are summarized in Table 1. Four types of topographic features, ray crater, crater with bright wall, crater with rough floor, and shadowed topography, presents as cold spots in the nighttime microwave map. However, they have shown different characters in the daytime microwave map and the nighttime infrared map. These characters give us clues to reveal the underlying physical mechanism of thermal anomalies.

Table 1. Classification and the performance of thermal anomalies in the MW and IR observation.

ΔTB	ray crater	crater with bright wall	crater with rough floor	shadowed topography	others
IR _{night}	Hot spot	Hot spot	Hot spot	Cold spot	Cold /hot spot
MW _{night}	Cold spot	Cold spot	Cold spot	Cold spot	Cold /hot spot
MW _{day}	Cold /hot spot	Cold spot	Hot spot	Cold spot	Cold /hot spot
Total	103	22	21	71	49

References: [1] Pettit E and Nicholson S. B. (1930) *J. Astrophys.*, (71), 102-135. [2] Shorthill R. W and Saari J. M. (1965) *Science*, 150(3693), 210-212. [3] Fudali R. F. (1966) *Icarus*, 5(1-6), 536-544. [4] Saari J. M. Shorthill R. W. and Deaton T. K. (1966) *Icarus*, 5, 635-659. [5] Buhl D. Welch W. J. and Rea D.G. (1968) *JGR*, 73(24), 7593-7608. [5] Hunt G. R. Salisbury J. W. and Vincent R. K. (1968) *Science*, 162, 252-254. [6] Paige D. A. Williams J. P. Sullivan M. T and Greenhagen B. T. (2011) *LPSC Abstracts*. [7] Chan K. L. Tsang K. T. Kong B. and Zheng Y. C. (2010) *Earth and Planetary Science Letters*, 295(1-2), 287-291. [8] Zheng Y. C. Tsang K. T. Chan K. L. Zou Y. L. Zhang F. and Ouyang Z. Y. (2012) *Icarus*, 219(1), 194-210.

Acknowledgements: This work is supported by the Sci. & Tech. Develop. Fund in Macao SAR (048/2012/A2), NSFC program (40904051), CAS program (XDA040 71900), and Hong Kong Scholar Program.